

Discovery of a 2,4-Disubstituted Pyrrolo-[1,2-*f*][1,2,4]triazine Inhibitor (BMS-754807) of Insulin-like Growth Factor Receptor (IGF-1R) Kinase in Clinical Development[†]

Mark D. Wittman,^{*,‡} Joan M. Carboni,[‡] Zheng Yang,[#] Francis Y. Lee,[‡] Melissa Antman,[∞] Ricardo Attar,[‡] Praveen Balimane,[#] Chiehying Chang,[×] Cliff Chen,[‡] Lorell Discenza,[‡] David Frennesson,[‡] Marco M. Gottardis,[‡] Ann Greer,[‡] Warren Hurlburt,[‡] Walter Johnson,[‡] David R. Langley,[§] Aixin Li,[‡] Jianqing Li,^{||} Peiyang Liu,[‡] Harold Mastalerz,[‡] Arvind Mathur,[●] Krista Menard,[‡] Karishma Patel,[#] John Sack,[×] Xiaopeng Sang,[‡] Mark Saulnier,[‡] Daniel Smith,^{||} Kevin Stefanski,[∞] George Trainor,[◆] Upender Velaparthy,[‡] Guifen Zhang,[‡] Kurt Zimmermann,[‡] and Dolatrai M. Vyas[‡]

[‡]Discovery Chemistry and [§]Macromolecular Structure and ^{||}Department of Chemical Synthesis and Bristol-Myers Squibb Co., 5 Research Parkway, Wallingford, Connecticut 06492, [‡]Oncology Drug Discovery and [#]Metabolism and Pharmacokinetics and [×]Macromolecular Structure and [∞]Pharmaceutics and [●]Department of Chemical Synthesis and [◆]Discovery Chemistry, Bristol-Myers Squibb Co., Route 206 and Province Line Road, Princeton, New Jersey 08540

Received June 2, 2009

Abstract: This report describes the biological activity, characterization, and SAR leading to **9d** (BMS-754807) a small molecule IGF-1R kinase inhibitor in clinical development.

Oncology drug discovery efforts have advanced a number of small molecule kinase inhibitors into clinical investigation. Among previously unexploited targets, small molecule inhibitors of insulin-like growth factor (IGF-1R^a) are advancing into clinical research. The interest in IGF-1R stems from the early recognition of the mitogenic properties of insulin.¹ These observations and the efficacy data for an IGF-1R specific antibody² and epidemiological findings³ have positioned IGF-1R among the emerging cell signaling pathways currently being explored.

IGF-1R plays an important role in tumor cell growth and survival. Upon stimulation with the ligand IGF-1 or IGF-2,

IGF-1R phosphorylates tyrosine residues on two major substrates, IRS-1 and Shc, which subsequently signal through the Ras/MAPK pathway and the PI3K/AKT/mTOR pathway.^{4,5} IGF-1R signaling affects cell proliferation, differentiation, migration, and regulation of the apoptotic machinery. The crosstalk observed between EGFR and IGF-1R signaling suggests the potential of IGF-1R inhibitors in combination with other targeted agents, cytotoxics, and radiation therapy.⁶ IGF-1R activation has also been implicated in the development of resistance toward trastuzumab treatment in breast⁷ and lung⁸ cancer.

Clinical proof of concept has been demonstrated with monoclonal antibodies directed against the extracellular ligand binding domain of the receptor. Small molecule IGF-1R inhibitors are just beginning to be explored, including OSI-906 (**1**)^{9,10} and a novel pyrrolo[1,2-*f*][1,2,4]triazine based inhibitor, BMS-754807 (**9d**), described herein.

Screening a series of kinase-focused libraries identified pyrazolopyrimidine **2** as a modest inhibitor of IGF-1R and the closely related insulin receptor (IR). Several other library members also had modest activity. Examination of their structure revealed the aminopyrazole element was common among the active members. X-ray crystal structures of some of the early analogues confirmed that the aminopyrazole forms a donor/acceptor/donor triad with the hinge region (Met1052 and Glu1050; see Figure 4). Since the pyrazolopyrimidine scaffold is a very common element in many ATP-competitive kinase inhibitors, we elected to transport the aminopyrazole binding motif onto the less common pyrrolo[1,2-*f*][1,2,4]triazine scaffold. This provided compounds that retained the IGF-1R potency of the screening lead. Some preliminary SAR was generated by varying the C-2 amine and alkyl substitution of the pyrazole. These efforts identified the C-2 pyrrolidine and the C-4 cyclopropylamino-pyrazole (Figure 1, **3**) as preferred groups for further optimization.

The general synthetic route used to prepare these molecules is illustrated in Scheme 1. Starting from the dichloropyrrolo-triazine **4**, treatment with 5-cyclopropyl-3-aminopyrazole resulted in the preferential displacement of the C-4 chloride. Microwave heating of **5** with the potassium salt of (*S*)-proline provided acid **6**. Amides **8a–g** were prepared using standard amide formation conditions. Significant racemization was observed in the formation of amides **8f** and **8g** due to the low nucleophilicity of the heterocyclic amines. Individual enantiomers were chromatographically separated and tested. To block this racemization, the (*S*)-2-methyl group was installed. Coupling of the chloride **5** with the potassium salt of (*S*)-2-methylproline under microwave heating provided the acid **7** from which the corresponding amides **9a–d** were prepared.

The primary amide **8a** has good IGF-1R potency and cell activity in the IGF-Sal derived cell line (see Table 1).¹¹ Previous compounds with modest IGF-1R potency and strong CDK2E inhibition also exhibit an antiproliferative response in the IGF-Sal cell line, so it could not be conclusively determined that CDK2E inhibition was not contributing to the cellular (antiproliferative) potency observed for **8a**.

[†]Coordinates of **9d** cocrystallized with IGF-1R have been submitted to the RCSB Protein Data Bank (PDB code 3I81).

*To whom correspondence should be addressed. Phone: (203) 677-6318. Fax: 203-677-7702. E-mail: mark.wittman@bms.com.

^aAbbreviations: IGF-1R, insulin-like growth factor receptor 1; SAR, structure–activity relationship; IGF-1, insulin-like growth factor 1; IGF-2, insulin-like growth factor 2; IRS-1, insulin receptor substrate 1; Shc, Src homology containing adapter protein; MAPK, mitogen-activated protein kinase; PI3K, phosphatidylinositol 3-kinase; mTOR, mammalian target of rapamycin; EGFR, epidermal growth factor receptor; IR, insulin receptor; CDK2E, cyclin-dependent kinase 2E; NMP, 1-methyl-2-pyrrolidinone; PyBOP, (benzotriazol-1-yloxy)tripyrrolidinophosphonium hexafluorophosphate; HOBt, 1-hydroxybenzotriazole; PEG400, poly(ethylene glycol) 400; pIGF-1R, phospho-IGF-1R; pAKT, phospho-AKT; PAMPA, parallel artificial membrane permeability; PK, pharmacokinetics; CYP, cytochrome P-450; PD, pharmacodynamic.

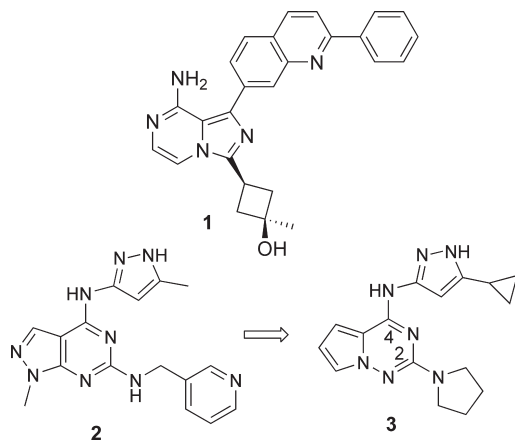
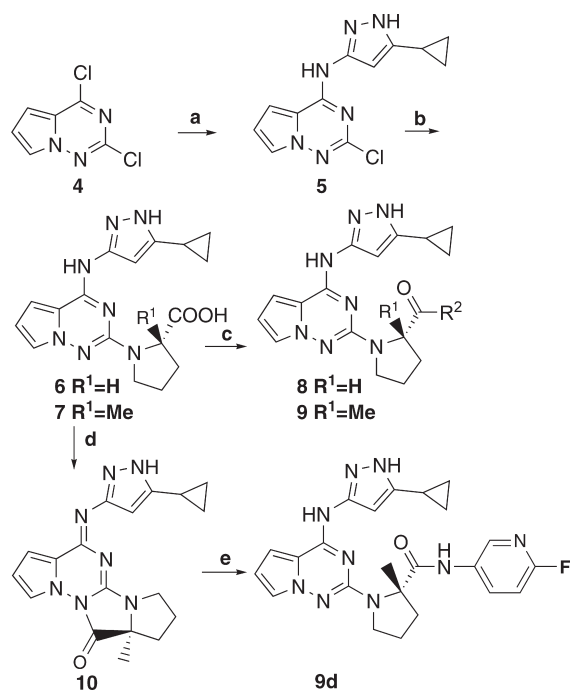


Figure 1. New IGF-1R lead chemotypes.

Scheme 1. General Synthetic Scheme^a



^a (a) 5-Cyclopropyl-3-aminopyrazole, EtN(*i*-Pr)₂, *i*-PrOH; (b) (*S*)-proline or (*S*)-2-methylproline, KO-*t*-Bu, NMP, 170 °C, microwave; (c) PyBOP, HOBT, amine; (d) SOCl₂, DMF, 50 °C; (e) 3-amino-6-fluoropyridine, 50–25 °C, 20 h (71% for two steps).

The enantiomeric amide **8b**, prepared using (*R*)-proline, is 5-fold less potent vs IGF-1R with a similar loss in cell potency. The change in stereochemistry did not impact kinase selectivity. Substitution of the (*S*)-amide increased the potency and selectivity for IGF-1R (it is noted that all of the analogues described also inhibit the related IR with equal potency). Aromatic and heterocyclic amides improve the potency for IGF-1R and the kinase selectivity (**8c–g**). The importance of the secondary amide is noted with the lack of activity observed for the *N*-methyl analogue **8e**. The pyridylamide **8g** has similar IGF-1R potency to the thiazole analogue **8f** with improved cell activity and kinase selectivity vs CDK2E and other kinases. The corresponding (*S*)-2-methyl analogues **9a** and **9b** retain potency with improved kinase selectivity and cell activity in comparison to the proline derivatives **8f** and **8g**. Optimization of the pyridyl substitution of the 3-pyridyl

Table 1. SAR of Proline Amide

	R ¹	R ²	IGF-1R ^a	CDK2E ^a	IGF-Sal ^b
8a	H (<i>S</i>)	NH ₂	41	2	47
8b	H (<i>R</i>)	NH ₂	199	24	310
8c	H (<i>S</i>)	NHPh	13	322	133
8d	H (<i>S</i>)	NH(4-Me-Ph)	40	1422	426
8e	H (<i>S</i>)	NMePh	717	200	
8f	H (<i>S</i>)	2-NH-thiazole	2	40	69
8g	H (<i>S</i>)	3-NH-pyridine	9	577	39
9a	Me (<i>S</i>)	2-NH-thiazole	4	329	67
9b	Me (<i>S</i>)	3-NH-pyridine	6	1432	24
9c	Me (<i>S</i>)	2-pyrazine	3	897	1
9d	Me (<i>S</i>)	3-NH-6-F-pyridine	2	1035	7

^a All data reported are for stereochemically pure enantiomers and IC₅₀ values reported in nM and are determined with ATP concentration of K_m for each kinase.¹² ^b Cell activity measured by [³H]thymidine incorporation after 72 h of exposure. The IGF-Sal cell line is derived from spontaneous tumors in transgenic mice that overexpress a constitutively activated IGF-1R and as such is very sensitive to IGF-1R inhibitors relative to inhibitors of other kinases.¹¹

Table 2. Mouse PK/Efficacy Screen^a

	R ¹	R ²	% TGI ¹³	MED ^b	Δ wt ^c (g)
9a	Me	2-NH-thiazole	74	12.5	0.3
9b	Me	3-NH-pyridine	76	25	1.9
9c	Me	2-pyrazine	113	6.25	-3.6
9d	Me	3-NH-6-F-pyridine	102	6.25	0.2

^a Compounds dosed orally bid in 80/20 PEG400/water. ^b Minimum effective dose in mg/kg, the lowest dose at which an efficacious result is achieved. ^c Change in body weight between the treated and untreated groups at 25 mg/kg dose. Weight loss of > 1 g represents a 5% loss in total body weight over 5 days and was generally considered indicative of the maximum tolerated dose.

analogue **9b** was also investigated. The 6-fluoro-3-pyridyl analogue **9d** provides the optimal balance of potency, cell activity, and selectivity.

Compound **9d** inhibits the phosphorylation of IGF-1R (IC₅₀ = 13nM) and the downstream targets Akt (IC₅₀ = 22nM) and MAPK (IC₅₀ = 13nM) in the IGF-Sal cell line with IC₅₀ consistent with the antiproliferative IC₅₀ (7 nM) in this cell line. These data provide confidence that the observed antiproliferative effect is due to IGF-1R inhibition.

In a traditional medicinal chemistry approach, exposure data are collected and together with cellular potency decisions are made on which analogues to advance to efficacy testing. To accelerate the lead optimization of this pyrrolotriazine series, an alternative strategy was developed. Since the transgenic-derived IGF-Sal tumor model¹¹ has a very rapid tumor doubling time (2 days), it was possible to conduct an oral PK/efficacy screen in mice. By inclusion of doses of 6, 12, and 25 mg/kg b.i.d., an efficacy and tolerability readout could be obtained within 5 days from the initiation of the experiment. Guided by cellular potency, *in vitro* permeability, and metabolic stability data, *in vivo* active compounds were quickly identified (see Table 2). Among the compounds of interest were **9a–d**. Compounds **9c** and **9d** achieved complete tumor growth inhibition¹³ at the 6.25 mg/kg dose. Compound **9c** showed signs of toxicity at the 25 mg/kg dose with greater than 2 g of weight loss observed (> 10% body weight loss over 5 days). Compound **9d** was identified with strong efficacy in the IGF-Sal tumor model with minimal weight loss at the upper dose and was chosen for further characterization.

A dose response study was conducted in the IGF-Sal tumor model, and **9d** was found to be active at doses from 3 mg/kg upward. Tumor samples were collected 2 h after final dose and

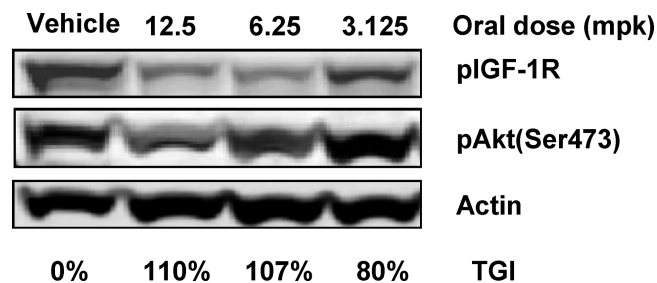


Figure 2. Dose response and target inhibition in the IGF-Sal tumor model following oral dosing of **9d**.

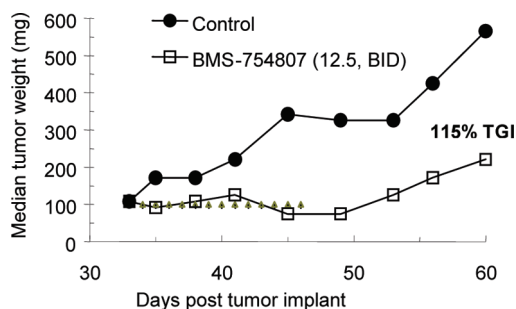


Figure 3. Rh41 efficacy for **9d**. Compound was administered on a twice daily schedule for 14 days represented by the diamonds. The compound was administered as a solution in PEG400/water (80:20 v/v) vehicle.

analyzed for inhibition of pIGF-1R and pAKT.¹⁴ Inhibition of pIGF-1R and pAKT showed a dose response that correlated with % TGI (see Figure 2). Efficacy was also observed in the IGF-1R dependent rhabdomyosarcoma model (see Figure 3), Rh41, and in other xenograft models.¹⁵

An optimized synthesis of **9d** is illustrated in Scheme 1. The (*S*)-2-methylproline acid **7** could be activated with thionyl chloride to provide the cyclic urea **10** which was directly reacted with 3-amino-6-fluoropyridine to provide **9d** in 71% yield from acid **7**.

The crystal structure of **9d** cocrystallized with the kinase domain of IGF-1R is shown in Figure 4. Key features include the donor/acceptor/donor hydrogen bond triad with Met1052 and Glu1050 within the hinge region of the kinase. The cyclopropyl group occupies the shallow “gatekeeper” region of the kinase, with the fluoropyridylamide extending into the sugar pocket. In this crystal structure R1127, D1128, and I1129 are not well-defined, indicating flexibility in the P-loop of the kinase.

The kinase selectivity of **9d** was evaluated by screening against a number of in-house kinases. In addition to IGF-1R and IR, *in vitro* kinase activity was noted for AurB, Axl, Met, Ron, and TrkA/B although the functional effects of inhibiting these kinases in cells were much less pronounced than the effect observed for inhibition of IGF-1R.¹⁵

The protein binding for **9d** ranges from of 98.5% in mouse plasma to 95.9% in human plasma. This compound is highly permeable in the PAMPA assay (387–713 nm/s, pH 7.4) and in Caco-2 cells (141–161 nm/s), suggesting the compound is well-absorbed. Moderate to good bioavailability in rats and dogs is observed where clearance is moderate to low (Table 3). However, in mouse and monkey, high clearance contributes to poor bioavailability. Despite the high clearance and low bioavailability in mice, a sufficient concentration of **9d** could be achieved to provide efficacy presumably due the high

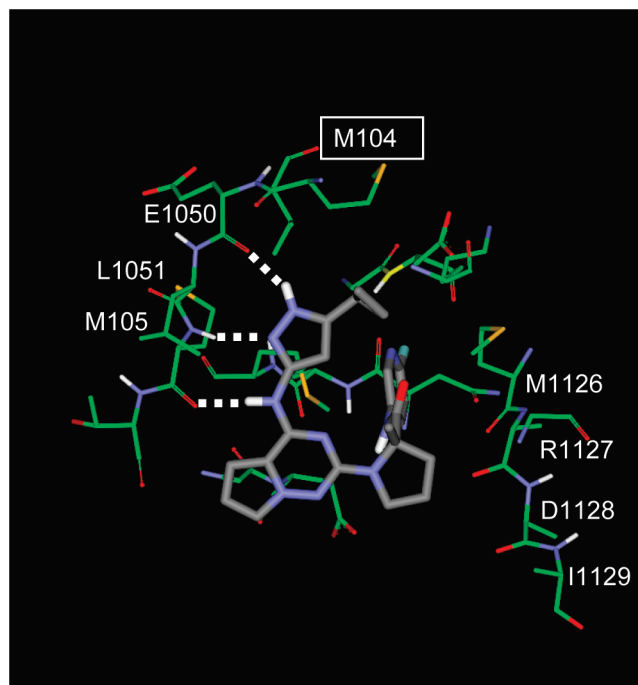


Figure 4. X-ray crystal structure of **9d** cocrystallized with IGF-1R (RCSB Protein Data Bank PDB code 3I81).

Table 3. Average Clearance and Bioavailability among Species^a

	CL _{tot} ((mL/min)/kg)	F (%)
mouse	113	6
rat	20	30
dog	3.5	59
monkey	41	8

^aClearances were determined after *iv* administration. Compound was administered as a solution in PEG400/water (80:20 v/v).

permeability and potency of the compound. The species-dependent clearances and oral bioavailabilities make the prediction of the human dose challenging. However, even with the “worst case” scenario of human PK being similar to monkey (high clearance, low bioavailability), the projected human efficacious dose was still reasonable (< 500 mg/day). A full complete discussion of the PK/efficacy relationship will be reported elsewhere.

Compound **9d** was run through a battery of preclinical safety assays (Table 4). No significant ion channel activity, CYP inhibition, hepatotoxicity (> 50 μM), or genotoxicity (Ames negative) was observed, and broad based pharmacological profiling did not reveal any off-target activities.

Table 4. Ion Channel and CYP Inhibition IC₅₀

ion channel	IC ₅₀ (μM)	CYP inhibition	IC ₅₀ (μM)
hERG	> 10	CYP3A4 (BzR)	> 40
L-type Ca ²⁺	> 10	CYP3A4 (BFC)	7
Na ⁺	> 10	CYP2C19	11
		CYP2C9	23
		CYP2D6	> 40
		CYP1A2	> 40

In summary, the pyrrolo[1,2-*f*][1,2,4]triazine chemotype was optimized for IGF-1R potency, selectivity, and safety to provide the clinical candidate **9d**. In preclinical animal safety studies elevation of glucose and insulin levels was observed at doses that exceeded an efficacious exposure presumably due to concomitant inhibition of the insulin receptor. Initial human

PK indicates that human clearances are low and good bioavailability has been observed. The full biological profile,¹⁵ PK/PD studies, and further clinical studies of **9d** will be presented in due course.

Acknowledgment. The authors thank Gordon Todderud and the Lead Evaluation group at BMS for generating the kinase data presented in Table 1 and the Lead Profiling Department at BMS for generating the data presented in Table 4.

Supporting Information Available: Procedure for the preparation of **9d**, analytical data, and procedures for in vitro and in vivo assays. This material is available free of charge via the Internet at <http://pubs.acs.org>.

References

- (1) Salmon, W. D.; Daughaday, W. H. A hormonally controlled serum factor which stimulates sulfate incorporation by cartilage in vitro. *J. Lab. Clin. Med.* **1957**, *49*, 825–836.
- (2) Arteaga, C. L.; Kitten, L. J.; Coronado, L. J.; Jacobs, S.; Kull, F. C., Jr.; Allred, D. C.; Osborne, C. K. Blockade of the type I somatomedin receptor inhibits growth of human breast cancer cells in athymic mice. *J. Clin. Invest.* **1989**, *84*, 1418–1423.
- (3) Chan, J. M.; Stampfer, M. J.; Giovannucci, E.; Gann, P. H.; Ma, J.; Wilkinson, P.; Hennekens, C. H.; Pollak, M. Plasma insulin-like growth factor-I and prostate cancer risk: a prospective study. *Science* **1998**, *279*, 563–566.
- (4) Skolnik, E. Y.; Lee, C. H.; Batzer, A.; Vicentini, L. M. The SH2/SH3 domain-containing protein GRB2 interacts with tyrosine-phosphorylated IRS1 and Shc: implications for insulin control of ras signaling. *EMBO J.* **1993**, *12*, 1929–1936.
- (5) Vanhaesebroeck, B.; Alessi, D. R. The PI3K-PDK1 connection: more than just a road to PKB. *Biochem. J.* **2000**, *346*, 561–576.
- (6) Buck, E.; Eyzaguirre, A.; Rosenfeld-Franklin, M.; Thomson, S.; Mulvihill, M.; Barr, S.; Brown, E.; O'Connor, M.; Yao, Y.; Pachter, J.; Miglarese, M.; Epstein, D.; Iwata, K. K.; Haley, J. D.; Gibson, N. W.; Ji, Q.-S. Feedback mechanisms promote cooperativity for small molecule inhibitors of epidermal and insulin-like growth factor receptors. *Cancer Res.* **2008**, *68*, 8322–8332.
- (7) Camirand, A.; Zakikhani, M.; Young, F.; Pollak, M. Inhibition of insulin-like growth factor-I receptor signaling enhances growth-inhibitory and proapoptotic effects of gefitinib (Iressa) in human breast cancer cells. *Breast Cancer Res.* **2005**, *7*, R465–R474.
- (8) Morgillo, F.; Woo, J. K.; Kim, E. S.; Hong, W. K.; Lee, H. Y. Heterodimerization of insulin-like growth factor receptor/epidermal growth factor receptor and induction of survivin expression counteract the antitumor action of erlotinib. *Cancer Res.* **2006**, *66*, 10100–10111.
- (9) Arnold, L. D.; Cesario, C.; Coate, H.; Crew, A. P.; Dong, H.; Foreman, K.; Honda, A.; Laufer, R.; Li, A.-H.; Mulvihill, K. M.; Mulvihill, M. J.; Nigro, A.; Panicker, B.; Steinig, A. G.; Sun, Y.; Weng, Q.; Werner, D. S.; Wyle, M. J.; Zhang, T. Patent Application WO2005/097800, **2005**.
- (10) Volk, B.; Buck, E.; Coate, H.; Cooke, A.; Dong, H.; Eyzaguirre, A.; Feng, L.; Foreman, K.; Rosenfeld-Franklin, M.; Kleinberg, A.; Landfair, D.; Mak, G.; Nigro, A.; O'Connor, M.; Pirritt, C.; Silva, S.; Siu, K.; Steinig, A.; Stolz, K.; Tavares-Greco, P.; Turton, R.; Werner, D.; Yao, Y.; Arnold, L.; Gibson, N. W.; Pachter, J. A.; Wild, R.; Ji, Q.-S.; Mulvihill, M. J. OSI-906: A Novel, Potent, and Selective First-in-Class Small Molecule Insulin-like Growth Factor 1 Receptor (IGF-1R) Inhibitor in Phase I Clinical Trials. *Abstracts of Papers*, 238th National Meeting of the American Chemical Society, Washington, DC, August 16–20, 2009; MEDI-152.
- (11) Carboni, J. M.; Lee, A. V.; Hadsell, D. L.; Rowley, B. R.; Lee, F. Y.; Bol, D. K.; Camuso, A. E.; Gottardis, M.; Greer, A. F.; Ho, C. P.; Hurlburt, W.; Li, A.; Saulnier, M.; Velaparthi, U.; Wang, C.; Wen, M.-L.; Westhouse, R. A.; Wittman, M.; Zimmermann, K.; Rupnow, B. A.; Wong, T. W. Tumor development by transgenic expression of a constitutively active insulin-like growth factor I receptor. *Cancer Res.* **2005**, *65*, 3781–3787.
- (12) The ATP concentration at K_m provided the most sensitive inhibitor response where the IC_{50} approximates the K_i (within $2\times$).
- (13) $\% TGI = [(tumor\ size\ of\ control\ group\ at\ end\ of\ treatment) - (tumor\ size\ of\ treated\ group\ at\ the\ end\ of\ treatment)] / [(tumor\ size\ of\ control\ group\ at\ the\ start\ of\ treatment) - (tumor\ size\ of\ control\ group\ at\ the\ end\ of\ treatment)]$. $\% TGI > 50\%$ is considered active. Each treatment group consisted of 6 mice. Tumors were measured on day 0 and day 4.
- (14) Mice were dosed orally with **9d** at 3.125, 6.25, and 12.5 mg/kg b.i.d. for 4 days. On day 5, a final dose of compound was administered to mice and the tumors were excised after 2 h. The effect of **9d** on pIGF-1R and pAkt activity was monitored by Western blot analysis using antibodies specific to IGF-1R and Akt.
- (15) Carboni, J. M.; Wittman, M.; Yang, Z.; Lee, F.; Greer, A.; Hurlburt, W.; Hillerman, S.; Cao, C.; Cantor, G.; Chen, C.; Discenza, L.; Menard, K.; Li, A.; Trainor, G.; Vyas, D.; Kramer, R.; Attar, R.; Gottardis, M. BMS-754807, a small molecule inhibitor of IGF-1R/IR. *Mol. Cancer Ther.*, in press.